Author Manuscript

Author Manuscript

Author Manuscript

Author Manuscript

HHS Public Access

Author manuscript

J Steroid Biochem Mol Biol. Author manuscript; available in PMC 2015 June 14.

Published in final edited form as:

J Steroid Biochem Mol Biol. 2015 April ; 148: 138–147. doi:10.1016/j.jsbmb.2014.11.005.

Suppression of epithelial ovarian cancer invasion into the omentum by 1α,25-dihydroxyvitamin D_3 and its receptor

Panida Lungchukiet[a], **Yuefeng Sun**[a], **Ravi Kasiappan**[a], **Waise Quarni**[a], **Santo V. Nicosia**[a,b,d], **Xiaohong Zhang**[a,b,c], and **Wenlong Bai**[a,b,c,*]

[a]The Departments of Pathology and Cell Biology, University of South Florida, H. Lee Moffitt Cancer Center, 12901 Bruce B. Downs Blvd., MDC 64, Tampa, FL 33612-4799, USA

[b]Oncological Sciences, H. Lee Moffitt Cancer Center, University of South Florida, 12901 Bruce B. Downs Blvd., MDC 64, Tampa, FL 33612-4799, USA

[c]University of South Florida College of Medicine, and Programs of Cancer Biology & Evolution, H. Lee Moffitt Cancer Center, 12901 Bruce B. Downs Blvd., MDC 64, Tampa, FL 33612-4799, USA

[d]Chemical Biology and Molecular Medicine, University of South Florida, H. Lee Moffitt Cancer Center, 12901 Bruce B. Downs Blvd., MDC 64, Tampa, FL 33612-4799, USA

Abstract

Epithelial ovarian cancer (EOC) is the leading cause of gynecological cancer death in women, mainly because it has spread to intraperitoneal tissues such as the omentum in the peritoneal cavity by the time of diagnosis. In the present study, we established *in vitro* assays, *ex vivo* omental organ culture system and syngeneic animal tumor models using wild type (WT) and vitamin D receptor (VDR) null mice to investigate the effects of 1α,25-dihydroxyvitamin D_3 ($1,25D_3$) and VDR on EOC invasion. Treatment of human EOC cells with $1,25D_3$ suppressed their migration and invasion in monolayer scratch and transwell assays and ability to colonize the omentum in the *ex vivo* system, supporting a role for epithelial VDR in interfering with EOC invasion. Furthermore, VDR knockdown in OVCAR3 cells increased their ability to colonize the omentum in the *ex vivo* system in the absence of $1,25D_3$, showing a potential ligand-independent suppression of EOC invasion by epithelial VDR. In syngeneic models, ID8 tumors exhibited an increased ability to colonize omenta of VDR null over that of WT mice; pre-treatment of WT, not VDR null, mice with EB1089 reduced ID8 colonization, revealing a role for stromal VDR in suppressing EOC invasion. These studies are the first to demonstrate a role for epithelial and stromal VDR in mediating the activity of $1,25D_3$ as well as a $1,25D_3$-independent action of the VDR in suppressing EOC invasion. The data suggest that VDR-based drug discovery may lead to the development of new intervention strategies to improve the survival of patients with EOC at advanced stages.

© 2014 Elsevier Ltd. All rights reserved.

*Corresponding author at: The Departments of Pathology and Cell Biology, University of South Florida, H. Lee Moffitt Cancer Center, 12901 Bruce B. Downs Blvd., MDC 64, Tampa, FL 33612-4799, USA. Tel.: +1 813 974 0563; fax: +1 813 974 5536. wbai@health.usf.edu (W. Bai).

Conflicts of interest

The authors have no conflicts of interest to report.

Author Manuscript Author Manuscript Author Manuscript Author Manuscript

This article is part of a Special Issue entitled “Vitamin D Workshop”.

Keywords

1,25-Dihydroxyvitamin D_3; Omentum; Vitamin D receptor; Ovarian cancer; Tumor invasion

1. Introduction

EOC is the deadliest among all gynecologic cancers and causes more deaths than cervical and uterine cancers combined. Despite the overall advancement in cancer research and clinical development over recent decades, there has been little improvement in EOC mortality rates. The poor prognosis is mainly due to the disease reaching an advanced stage before it is discovered. Primary cytoreductive surgery followed by chemotherapy with cisplatin and paclitaxel is the standard treatment regimen for patients with advanced EOC, yielding high response rates and improving both short and medium-term survivals. However, most patients will eventually relapse and die of their cancer [32]. Intervention strategies that suppress EOC invasion would retain the cancer inside ovaries, allowing simple surgery to suffice as a cure.

Omentum is a sheet-like tissue attached to the greater curvature of the stomach. It is the most common site for EOC metastatic spread [19,20,36]. The spread happens rather quickly and, in 80% of EOC patients, the cancer usually has spread to this tissue at the time of diagnosis. The composition and function of omenta are similar between mice and human. They contain primarily adipose tissue and islands of compact immune cells called milky spots, which is a lymphoid organ controlling peritoneal cavity immune response [33]. A recent study has reported that omental adipocytes promote EOC metastasis by providing energy for rapid tumor growth [30]. Nevertheless, the mechanisms underlying EOC invasion into the omentum are largely unknown and key molecular events controlling the process remain to be defined.

$1,25D_3$ is a fat-soluble seco-steroid hormone best known for its role in calcium and phosphate homeostasis. Effects of $1,25D_3$ are mediated through the VDR that belongs to the steroid/thyroid hormone receptor superfamily [9,39]. In addition, $1,25D_3$ and its analogs elicit anti-tumor effects in a wide variety of cancer cell types through the induction of cell death, cell cycle arrest, differentiation, angiogenesis, etc. [3,6,7,11,12,37,38,40,41,45], suggesting that $1,25D_3$ holds great promise in cancer intervention. In EOC cells, $1,25D_3$ causes cell cycle arrest at the G2/M transition through p53-independent induction of GADD45 [16]. Further studies have identified p27 as the key mediator of $1,25D_3$-induced growth arrest in G1/S checkpoint [23] and defined a decrease in hTERT mRNA stability through microRNA as the mechanism underlying $1,25D_3$-induced cell death [15,17]. However, a role for $1,25D_3$ and VDR in EOC invasion and metastasis has not been investigated.

In the present studies, a series of experiments employing *in vitro*, *ex vivo* and *in vivo* EOC tumor models were conducted to assess the possible involvement of $1,25D_3$ and VDR in suppressing EOC invasion into the omentum. These studies have revealed a novel role for

Author Manuscript Author Manuscript Author Manuscript Author Manuscript

$1,25D_3$ in suppressing EOC invasion through both epithelial and stromal VDR. The findings suggest that VDR-based drug discovery may lead to a new intervention strategy to improve the clinical outcomes of patients with advanced EOC.

2. Materials and methods

2.1. Cell culture and reagents

OVCAR3 human ovarian carcinoma cells (American Type Culture Collection, Manassas, VA) were cultured in RPMI 1640 medium supplemented with 15% calf serum (CS), 2 mM L-glutamine, 50 units/ml penicillin, 50 μg/ml streptomycin, 10 mM HEPES,1 mM sodium pyruvate, 4.5 g/l glucose, 1.5 g/l sodium bicarbonate and 10 μg/ml bovine insulin. SKOV3-Luc cells, human ovarian carcinoma cell line, (Cell Biolabs, San Diego, CA) were maintained in DMEM containing 584 mg/l L-glutamine and 4.5 g/l glucose, supplemented with 5% CS, 100 units/ml penicillin, 100 μg/ml streptomycin and 500 μg/ml geneticin. ID8-VEGF murine ovarian cancer cells have been described elsewhere in detail [42]. The cells were generated by transfecting ID8 cells with a retroviral vector containing green fluorescent protein (GFP) and VEGF164, which accelerated tumor growth and ascites formation, significantly enhanced tumor angiogenesis, and substantially promoted the survival of tumor cells *in vivo* [35]. Cells were maintained in DMEM supplemented with 5% CS, 100 units/ml penicillin, and 100 μg/ml streptomycin.

$1,25D_3$ (calcitriol) was purchased from Calbiochem (La Jolla, CA). EB1089 (seocalcitol) was generously provided by Leo Pharmaceutical Products (Ballerup, Denmark). They were reconstituted in 100% ethanol (EtOH) and stored protected from light at −20 °C. All handling of $1,25D_3$ and EB1089 was performed with indirect lighting.

2.2. Stable transfections with luciferase and VDR short hairpin RNA (shRNA)

To establish cells stably expressing luciferase, OVCAR3 and ID8-VEGF cells were transfected with 1 μg of pGL3-control plasmid (Promega, Madison, WI) using Lipofectamine 2000 (Invitrogen, Grand Island, NY) following the protocol from Invitrogen. Stable transfectants were established after selection in medium containing 400 μg/ml (for OVCAR3-Luc) or 800 μg/ml (for ID8-VEGF-Luc) G418 for a period of about 4 weeks.

For the establishment of OVCAR3 cells stably expressing control or VDR shRNA, cells were transfected with 2 μg of control pFIV-H1-Puro vector or shVDR [26] using the Lipofectamine 2000 in 2 ml of Opti-MEM medium (Invitrogen, Grand Island, NY). 4 h post transfections, the cell were re-plated in RPMI medium containing 10% CS and 2 μg/ml puromycin for 48 h. Cells were then split and placed at low density. Stable clones were achieved through selection with 2 μg/ml puromycin for a period of about 4 weeks. Individual clones were isolated using glass cylinders. Two independent clones were analyzed and representative data were presented for each study.

2.3. Migration and invasion assays

Cell motility of OVCAR3 cells was assessed by the monolayer scratch assays. Cells were plated in 6-well plates in RPMI medium containing 5% CS. When the cells had reached

Author Manuscript Author Manuscript Author Manuscript Author Manuscript

confluence, the cell monolayer was scraped with a P200 pipette tip and rinsed with phosphate buffered saline (PBS) to dislodge cellular debris. The cells were then cultured in the medium containing EtOH, 10^{-7} or 10^{-8} M $1,25D_3$ for 0,1 and 2 days. Pictures were taken at different time points and cell motility was analyzed using the NIH image software (http://rsb.info.nih.gov/nih-image/Default.html) and presented as percentage of the change in distance between the edges of the scratch (relative to time zero). All assays were performed in triplicate and pictures from each culture were taken at 5 randomly chosen areas.

Cell migration and invasion assays using the transwell system from BD Bioscience (San Jose, CA) were performed following the manufacturer's instructions. In brief, cells were added to each transwell insert in serum-free media containing EtOH or 10^{-7} M $1,25D_3$ whereas, the medium in the lower chamber contained 10% CS. After incubation for 18 h at 37 °C, cells remaining in the insert were removed using cotton swabs. Cells migrated across the insert and attached to the under surface were fixed with 4% paraformaldehyde for 10 min and stained with 0.5% crystal violet. The amount of migrated cells was quantitatively assessed by reading the absorbance at 560 nm after re-dissolving the crystal violet staining in 10% acetic acid. Transwell cell invasion assays were performed similarly except that transwell inserts were pre-coated with growth factor-reduced Matrigel (BD Biosciences, San Jose, CA).

2.4. Animal breeding and maintenance

$VDR^{+/-}$ mice of C57B16 background (The Jackson Laboratory, Bar Harbor, ME) were mated to produce $VDR^{+/+}$ (WT), $VDR^{+/-}$ (HET) and $VDR^{-/-}$ (KO) mice. Twelve to sixteen-week old female mice were used for the experiments. Mice were weaned at 3 weeks of age and fed with a vitamin D – deficient rescued diet for VDR null mice (TD87095, Teklad, Madison, WI). The diet has been shown to normalize serum mineral homeostasis, bone growth and body weight in VDR null mice [21,24]. Mice were genotyped by PCR amplification of DNA isolated from tail snips. Three pairs of primers were used (5′-CAC GAG ACT AGT GAG ACG TG – 3′, 5′-CTC CAT CCC CAT GTG TCT TT – 3′, 5′-TTC TTC AGT GGC CAG CTC TT –3′) to amplify a 382 bp fragment for WT, 382 and 500 bp fragments for HET and a 500 bp fragment for KO mice. All procedures were reviewed and approved by the Institutional Animal Care and Use Committees at the University of South Florida.

2.5. *Ex vivo* co-culturing of mouse omenta with luciferase-marked human EOC cells

Cells were grown to 80% confluence and harvested. Harvested cells were washed twice with PBS and re-suspended at a concentration of 2×10^6 cells/ml in DMEM/F-12 (1:1) supplemented with 20% CS. Omenta were excised from eight to twelve-week old female mice and immediately attached to the membrane of Milicel culture inserts using Cell-Tak cell and tissue adhesive (BD Biosciences, San Jose, CA) as previously described [20]. Briefly, 6 μl of Cell-Tak was spread evenly on the transwell membrane. The membrane was then air-dried and washed twice with 500 μl of sterile water. One omentum per transwell was placed on the dried Cell-Tak coated membrane for 1 min without media. The transwell inserts with attached omenta were placed in a 12-well plate. 500 μl of cell suspension was

Author Manuscript Author Manuscript Author Manuscript Author Manuscript

transferred onto each omentum and 2.5 ml of DME/F-12 media was placed around the transwell. After co-culturing with the cell suspension for 24 h at 37 °C in a 5% CO_2 incubator, the omenta were then removed and washed three times with PBS. Omental tissue extracts were prepared and protein concentrations were determined using Bio-Rad protein assays (Bio-Rad Hercules, CA). Luciferase activity was measured using the Luciferase-Reporter Assay System (Promega, Madison, WI) according to the manufacturer's instructions in a luminometer (LMax II 384, Molecular Devices).

2.6. *In vivo* tumor inoculation and bioluminescence imaging

Sub-confluent ID8-VEGF-Luc cells were trypsinized, washed twice and collected by centrifugation at 1000 × *g* for 5 min. A single-cell suspension was prepared in PBS. 5×10^6 cells in a volume of 100 μl were inoculated into the mouse by intraperitoneal (*i.p.*) injection at time points indicated in the figure legends.

For imaging, mice were anesthetized with 2.5% isofluorene and administered an *i.p.* injection of 150 mg/g D-luciferin (Xenogen, Hopkinton, MA). 10 min after the luciferin injections, the omenta were dissected and placed in the Xenogen CCD imaging apparatus of the IVIS system (IVIS-200 series, Xenogen). Images were acquired and analyzed using Living Image Software (version 3,2, Xenogen).

2.7. Haematoxylin and eosin (H&E) stain, immunoblotting and immunohistochemical analyses

For immunoblotting analyses, proteins were separated in 10% SDS-PAGE and transferred onto immobilon membranes. Antibodies against VDR (S1882) (Epitomics, Burlingame, CA), α-actinin (sc-17829) (Santa Cruz Biotechnology, Dallas, Texas) and β-actin (sc-130300) (Santa Cruz Biotechnology, Dallas, Texas) were used at 1:1000, 1:1000 and 1:5000, respectively. Bound antibodies were detected using Pierce Chemiluminescent Detection Kit (Thermo Scientific, Rockford, Illinois).

For standard paraffin wax histology, tissues were excised and fixed overnight in 4% paraformaldehyde buffered in PBS (pH 7.4). Sections were cut and stained with hematoxylin and eosin using standard protocols. Stained sections were examined under light microscopy and images captured using CellSens™ system (Olympus America, Center Valley, PA). For immunohistochemistry, sections were deparaffinized and subjected to antigen retrieval. Endogenous peroxidase activity was quenched by incubation with 3% H_2O_2 for 5 min. VDR staining was performed using 9A7 antibody (ab8756) (Abcam, Cambridge, MA) diluted at 1:200. Visualization of the immunohistochemical reactions was carried out according to the DAKO EnVision+ system protocol (Dako North America, Carpinteria, CA).

2.8. Statistical analyses

The data are presented as means ± standard deviation (SD) with the number of observations (*n*) being indicated in the figure legends. Statistical comparisons were performed using the Student *t*-test. A value of $p < 0.05$ was considered to be statistically significant.

Author Manuscript Author Manuscript Author Manuscript Author Manuscript

3. Results

3.1. Suppression of human and mouse EOC migration and invasion by 1,25D$_3$ through epithelial VDR and its translation into *in vivo* suppression of EOC omental invasion in mice

In published microarray studies performed in OVCAR3 cells [44], a group of genes with known functions in regulating invasive behavior of cancer cells, including genes encoding extracellular matrix proteins and chemokines/cytokines, were identified as 1,25D$_3$ target genes, indicating a role for the hormone in controlling EOC invasion. To test this potential role, OVCAR3 cells were treated with vehicle or 1,25D$_3$ and the migration and invasion of the treated cells were assessed by monolayer scratch (Fig. 1A) and transwell (Fig. 1B) assays. It is clear from these studies that 1,25D$_3$ treatments suppressed OVCAR3 invasion and migration. More suppression was observed with 1,25D$_3$ at 10^{-7} than 10^{-8} M, showing a concentration-dependent effect of 1,25D$_3$ on EOC invasion through the VDR in epithelial cancer cells.

A recent study documented a technique to culture mouse omenta and visualize the omental colonization of cancer cells marked with GFP into the omentum [20]. To test whether the suppressive effect of 1,25D$_3$ on OVCAR3 cells can be translated into the suppression of EOC invasion into the omentum, the *ex vivo* system was employed and adapted to use OVCAR3 cells marked with luciferase to facilitate the accurate quantitation by simple luciferase assays (Fig. 2A and B). As shown in Fig. 2C, pre-treatments with 10^{-7} M 1,25D$_3$ significantly decreased the ability of OVCAR3-Luc cells to colonize mouse omenta in the *ex vivo* co-culture system as compared to vehicle treated cells. In this experiment, OVCAR3-Luc cells, not omenta, were treated with 1,25D$_3$, supporting the data from *in vitro* migration and invasion assays indicating that 1,25D$_3$ works through the VDR in the epithelial cancer cells to suppress EOC invasion.

To test whether the suppressive effects of 1,25D$_3$ on human EOC invasion are conserved in mouse ovarian tumor cells, ID8-VEGF mouse ovarian tumor cells were stably transfected with luciferase and treated with vehicle or 10^{-7} M 1,25D$_3$ for 6 days before being subjected to transwell migration and invasion analyses. As shown in Fig. 3A, the migration and invasion of ID8-VEGF-Luc cells were dramatically suppressed by 1,25D$_3$ treatments as compared to vehicle controls. More importantly, 1,25D$_3$ pre-treatments decreased the ability of ID8-VEGF-Luc cells to colonize mouse omenta after *i.p.* injection into intact mice (Fig. 3B). These studies show that the suppressive effects of 1,25D$_3$ on human EOC invasion observed in *in vitro* studies can be translated into *in vivo* suppression of omental colonization in syngeneic mouse ovarian tumor models.

3.2. 1,25D$_3$-independent suppression of EOC omental invasion by the VDR in the epithelial cancer cells

The finding that 1,25D$_3$ treatments suppress EOC invasion into the omentum raises the possibility that the VDR in the epithelial cancer cells may be a suppressor of EOC invasion. Indeed, SKOV3 cells which express little VDR as compared to OVCAR3 cells (Fig. 4A) exhibited a much stronger ability to invade mouse omentum in the *ex vivo* co-culturing assay

Author Manuscript Author Manuscript Author Manuscript Author Manuscript

system (Fig. 4B). The data suggest, though does not prove, a possible inverse correlation between VDR expression and EOC invasion.

To validate the suppressive role of the VDR in epithelial cancer cells, OVCAR3-Luc cells were stably transfected with control or VDR shRNA and the ability of the transfected cells to invade the omentum was compared in the *ex vivo* assay system. Immunoblotting analyses validated that the VDR shRNA decreased VDR protein expression as expected (Fig. 4C). In the *ex vivo* assay system, the luciferase activity in the omentum incubated with OVCAR3-Luc cells expressing VDR shRNA was significantly higher than that of cells incubated with the cells expressing control shRNA (Fig. 4D). The data provide the proof that the epithelial VDR in EOC cells is a suppressor of ovarian tumor invasion into the omentum. Since the *ex vivo* assays were performed in the absence of $1,25D_3$, the studies also reveal the existence of a $1,25D_3$-independent effect of the VDR in suppressing EOC invasion.

3.3. Suppression of EOC invasion by stromal VDR in the omentum

VDR is widely expressed in a number of cell types, including immune cells, adipocytes, microvascular cells and fibroblasts, which are the main components of omental stroma. Thus, the VDR in omental stroma may also play a role in suppressing EOC invasion and metastasis. To test this idea, the ability of OVCAR3-Luc and SKOV3-Luc to invade omenta isolated from WT and VDR null mice was first tested in the *ex vivo* assay system, followed by *in vivo* analyses using syngeneic mouse ovarian tumors established with ID8-VEGF-Luc cells. For each mouse used in the studies, the VDR status was validated by genotyping analyses (Fig. 5A). Immunoblotting (Fig. 5B) and immunohistochemical (Fig. 5C) analyses were also performed to validate that VDR protein expression levels were completely absent in omenta of VDR null mice.

In the *ex vivo* co-culturing assays, OVCAR3-Luc and SKOV3-Luc cells exhibited stronger ability to colonize omenta of VDR null mice than that of the WT (Fig. 5D), supporting a role of stromal VDR in the omentum in suppressing EOC invasion. Interestingly, the difference in the ability to colonize omenta of WT and VDR null mice was bigger for VDR-positive OVCAR3-Luc cells than VDR-negative SKOV3 cells, indicating the existence of a possible crosstalk between epithelial and stromal VDR.

Similar results were obtained in *in vivo* experiments in which ID8-VEGF-Luc cells were *i.p* injected into WT and VDR null mice and omenta removed for imaging analyses 18 h later. As shown in Fig. 6A, more ID8-VEGF cells colonized omenta of VDR null mice than that of the WT. H&E staining showed that the ID8-VEGF cells established metastatic tumors in the omentum in areas called milky spots (Fig. 6B). The data demonstrated that omenta in VDR null mice were more susceptible to EOC colonization as compared to that of the WT.

3.4. Suppression of EOC colonization to the omentum by EB1089 through the stromal VDR

To assess the effects of EB1089 on EOC colonization omenta through the stromal VDR, WT and VDR null mice were treated with vehicle (sesame oil) or EB1089 at 0.5 μg/kg every other day for 10 days prior to the *i.p* injection of ID8-VEGF-Luc cells. At 18 h post cell injection, luciferin was injected by *i.p.* and omenta were excised and subjected to luciferase

Author Manuscript Author Manuscript Author Manuscript Author Manuscript

imaging analyses. As shown in Fig. 7A, pre-treatment of WT mice with EB1089 significantly suppressed the colonization of ID8-VEGF-Luc cells into omenta. However, pre-treatments of VDR null mice with EB1089 did not suppress the colonization of ID8-VEGF-Luc cells into omenta in parallel analyses. The studies show that the $1,25D_3$ analog works through the stromal VDR to suppress EOC invasion.

4. Discussion

Understanding the mechanisms by which tumor cells become metastatic is of great significance in cancer biology and medicine for the simple reason that cancer mortality is often caused by metastatic rather than by primary tumors. The metastatic process requires that cells gain the ability to migrate and invade adjacent tissues to reach the vasculature and lymphatic system. In this study, we have investigated the potential role of $1,25D_3$ and VDR in suppressing EOC invasion into the omentum, the primary site for EOC invasion in patients. Our studies support the concept that $1,25D_3$ and its analog EB1089 suppress EOC invasion into the omentum through the cooperative actions of the VDR present in both the epithelial cancer cells and the stromal cells in the tumor microenvironment (Fig. 7B). This suppression is conserved between human and mouse EOC cells and is translatable into *in vivo* suppression of EOC invasion in mice. More importantly, the VDR exhibits a suppressive activity in the absence of $1,25D_3$, indicating the potential existence of a ligand-independent activity of the receptor in suppressing EOC invasion. Although it remains to be defined whether the suppressive activity of the VDR in the absence of $1,25D_3$ is truly ligand independent, the studies suggest that $1,25D_3$ and its synthetic analogs can be exploited to suppress EOC invasion and improve the survival of patients with EOC at advanced stages.

Our published studies have documented an important role for $1,25D_3$ and EB1089 in suppressing EOC growth in multiple human EOC cell lines both *in vitro* [15,16,23] and *in vivo* in mouse tumor models [17,18,43]. This study is the first to reveal a role for $1,25D_3$ in suppressing EOC invasion. The mechanisms underlying EOC growth suppression by $1,25D_3$ are relatively well-characterized. However, the molecular mechanisms by which $1,25D_3$ suppress EOC invasion remains to be defined. Our microarray analyses in OVCAR3 cells have identified a large number of genes encoding proteins with known functions in motility, tumor immunity, cell-cell and cell-extracellular matrix adhesion as $1,25D_3$ target genes [44]. It is rational to affirm that the suppression of EOC invasion by $1,25D_3$ would be mediated through one or more of these target genes. It would be important to define the essential genes that drive the suppression by small interference RNA approaches. In this regard, the *ex vivo* omental organ co-culturing system should provide a valuable assay system to validate the role of these identified target genes in EOC invasion.

The present studies with VDR null mice are also the first to define a role for the stromal VDR in mediating the suppression of EOC invasion by $1,25D_3$. The omentum is mainly comprised of adipocytes, immune cells, microvascular cells and fibroblasts, all of which are known to contribute to the EOC microenvironment. A role of omental adipocytes in supplying energy for EOC growth has been supported by a direct relationship between cancer cell growth and adipocyte depletion [30]. The peritoneal cavity is a unique immunological microenvironment. Numerous studies have demonstrated that EOC cells

Author Manuscript Author Manuscript Author Manuscript Author Manuscript

preferentially go to the milky spots [10,13,20,34], suggesting that the immune cells in the milky spots may provide a favorable microenvironment for the establishment of ovarian tumor metastasis. Furthermore, cancer associated fibroblasts (CAFs) are one of the most crucial components of the tumor microenvironment that promotes cancer invasion by various mechanisms. As shown in Fig. 5C, all of the cell types display the VDR and thus may be responsible for the suppression of omental metastases by $1,25D_3$.$1,25D_3$ actions in adipocytes [28], fibroblasts [5] and immune cells [14,27] have been reported in the literature. Elucidation of the molecular mechanism underlying the suppression of EOC invasion mediated through stromal VDR relies on the identification of the main cell types in omental tumor microenvironment that mediate the $1,25D_3$ action through the stromal VDR.

EB1089 is a $1,25D_3$ analog that is less calcemic than $1,25D_3$, but more potent than the natural VDR ligand in suppressing the growth of prostate [2,4,25,29], breast [8], colon [1,22] and retinoblastoma [31] tumors. Despite the promise of EB1089 shown in pre-clinical studies, attempts to translate these results to therapy in the clinics for other cancers have been disappointing to date. While the exact reasons for the disappointment remain unknown, it is possible that those clinical trials have been carried out with patient subjects whose tumors are insensitive to growth suppression by $1,25D_3$ and EB1089. Our published studies have shown that EB1089 suppressed the growth of OVCAR3 [43] and OV2008 [17] ovarian tumors in mice without causing hypercalcemia, suggesting that EOC is highly sensitive to $1,25D_3$ or EB1089 and thus trials with EOC patients may yield positive outcomes despite the disappointment in other cancers. Furthermore, our recent studies have shown that the administration of EB1089 suppressed EOC growth induced by a high-fat diet in mice [18]. Thus, selective recruitment of EOC patient subjects who are obese may improve the outcomes of clinical trials with $1,25D_3$ or EB1089.

In conclusion, the present studies support a new translational potential for $1,25D_3$ or its analogs in suppressing the invasive behavior of EOC. Since a $1,25D_3$-independent activity of the VDR in suppressing EOC invasion was also detected, compounds that regulate the $1,25D_3$-independent activity of the VDR or simply increase VDR expression will be potential drugs for EOC intervention. It is the ultimate goal of our future studies to fully define the mechanisms underlying the suppression of EOC invasion by epithelial and stromal VDR and to advance $1,25D_3$ or its analogs into clinics for the management of EOC growth, invasion and metastasis.

Acknowledgments

The authors would like to thank Ms. June Paciga for her assistance in conducting VDR immunohistochemistry, Dr. Takashi Tokono from Sapporo Medical University for providing VDR-shRNA and Dr. Weidong Xu from the University of South Florida for ID8-VEGF cells. We appreciate the technical support and assistance of the Tissue Core Facility, Moffitt Cancer Center. We also thank Mr. Clifford J. Webb for editorial input. The studies were supported by Public Health Service grants CA111334 (to Bai) and CA164147 (to Zhang) from the National Institutes of Health and a project as part of a program development grant from Ovarian Cancer Research Fund (to Bai).

Author Manuscript Author Manuscript Author Manuscript Author Manuscript

References

1. Akhter J, Chen X, Bowrey P, Bolton EJ, Morris DL. Vitamin D_3 analog, EB1089, inhibits growth of subcutaneous xenografts of the human colon cancer cell line, LoVo, in a nude mouse model. Dis Colon Rectum. 1997; 40:317–321. [PubMed: 9118747]
2. Bhatia V, Saini MK, Shen X, Bi LX, Qiu S, Weigel NL, Falzon M. EB1089 inhibits the parathyroid hormone-related protein-enhanced bone metastasis and xenograft growth of human prostate cancer cells. Mol Cancer Ther. 2009; 8:1787–1798. [PubMed: 19584236]
3. Bikle DD, Elalieh H, Welsh J, Oh D, Cleaver J, Teichert A. Protective role of vitamin D signaling in skin cancer formation. J Steroid Biochem Mol Biol. 2013; 136:271–279. [PubMed: 23059470]
4. Blutt SE, Polek TC, Stewart LV, Kattan MW, Weigel NL. A calcitriol analogue, EB1089, inhibits the growth of LNCaP tumors in nude mice. Cancer Res. 2000; 60:779–782. [PubMed: 10706079]
5. Campos LT, Brentani H, Roela RA, Katayama MLH, Lima L, Rolim CF, Milani C, Folgueira MAAK, Brentani MM. Differences in transcriptional effects of 1α,25-dihydroxyvitamin D_3 on fibroblasts associated to breast carcinomas and from paired normal breast tissues. J Steroid Biochem Mol Biol. 2013; 133:12–24. [PubMed: 22939885]
6. Chiang KC, Chen TC. Vitamin D for the prevention and treatment of pancreatic cancer. World J Gastroenterol. 2009; 15:3349–3354. [PubMed: 19610135]
7. Colston KW, Lowe LC, Mansi JL, Campbell MJ. Vitamin D status and breast cancer risk. Anticancer Res. 2006; 26:2573–2580. [PubMed: 16886666]
8. Colston KW, Mackay AG, James SY, Binderup L, Chander S, Coombes RC. EB1089: a new vitamin D analogue that inhibits the growth of breast cancer cells in vivo and in vitro. Biochem Pharmacol. 1992; 44:2273–2280. [PubMed: 1472092]
9. Evans RM, Mangelsdorf DJ. Nuclear receptors, RXR, and the Big Bang. Cell. 2014; 157:255–266. [PubMed: 24679540]
10. Gerber SA, Rybalko VY, Bigelow CE, Lugade AA, Foster TH, Frelinger JG, Lord EM. Preferential attachment of peritoneal tumor metastases to omental immune aggregates and possible role of a unique vascular microenvironment in metastatic survival and growth. Am J Pathol. 2006; 169:1739–1752. [PubMed: 17071597]
11. Ghous Z, Akhter J, Pourgholami MH, Morris DL. Inhibition of hepatocellular cancerbyEB1089: in vitro and in vive study. Anticancer Res. 2008; 28:3757–3761. [PubMed: 19189661]
12. Gonzalez-Sancho JM, Larriba MJ, Ordonez-Moran P, Palmer HG, Munoz A. Effects of 1alpha,25-dihydroxyvitamin D_3 in human colon cancer cells. Anticancer Res. 2006; 26:2669–2681. [PubMed: 16886677]
13. Hagiwara A, Takahashi T, Sawai K, Taniguchi H, Shimotsuma M, Okano S, Sakakura C, Tsujimoto H, Osaki K, Sasaki S, et al. Milky spots as the implantation site for malignant cells in peritoneal dissemination in mice. Cancer Res. 1993; 53:687–692. [PubMed: 8425204]
14. Hsu JW, Yin PN, Wood R, Messing J, Messing E, Lee YF. 1alpha,25-dihydroxylvitamin D_3 promotes Bacillus Calmette–Guerin immunotherapy of bladder cancer. Oncotarget. 2013; 4:2397–2406. [PubMed: 24353168]
15. Jiang F, Li Bao J, Nicosia P, Bai WSV. Induction of ovarian cancer cell apoptosis by 1,25-dihydroxyvitamin D_3 through the down-regulation of telomerase. J Biol Chem. 2004; 279:53213–53221. [PubMed: 15485861]
16. Jiang F, Li P, Fornace AJ Jr, Nicosia SV, Bai W. G2/M arrest by 1,25-dihydroxyvitamin D_3 in ovarian cancer cells mediated through the induction of GADD45 via an exonic enhancer. J Biol Chem. 2003; 278:48030–48040. [PubMed: 14506229]
17. Kasiappan R, Shen Z, Tse AK, Jinwal U, Tang J, Lungchukiet P, Sun Y, Kruk P, Nicosia SV, Zhang X, et al. 1,25-Dihydroxyvitamin D_3 suppresses telomerase expression and human cancer growth through microRNA-498. J Biol Chem. 2012; 287:41297–41309. [PubMed: 23055531]
18. Kasiappan R, Sun Y, Lungchukiet P, Quarni W, Zhang X, Bai W. Vitamin D suppresses leptin stimulation of cancer growth through microRNA. Cancer Res. 2014
19. Kenny HA, Dogan S, Zillhardt M, Yamada KM, Krausz SD, Lengyel T. Organotypic models of metastasis: a three-dimensional culture mimicking the human peritoneum and omentum for the

Author Manuscript Author Manuscript Author Manuscript Author Manuscript

study of the early steps of ovarian cancer metastasis. Cancer Treat Res. 2009; 149:335–351. [PubMed: 19763444]

20. Khan SM, Funk HM, Thiolloy S, Lotan TL, Hickson J, Prins GS, Drew AF, Rinker-Schaeffer CW. In vitro metastatic colonization of human ovarian cancer cells to the omentum. Clin Exp Metastasis. 2010; 27:185–196. [PubMed: 20229256]
21. Kovacs CS, Woodland ML, Fudge NJ, Friel JK. The vitamin D receptor is not required for fetal mineral homeostasis or for the regulation of placental calcium transfer in mice. Am J Physiol Endocrinol Metab. 2005; 289:E133–E144. [PubMed: 15741244]
22. Larriba MJ, Valle N, Palmer HG, Ordonez-Moran P, Alvarez-Diaz S, Becker KF, Gamallo C, de Herreros AG, Gonzalez-Sancho JM, Munoz A. The inhibition of Wnt/beta-catenin signalling by 1alpha,25-dihydroxyvitamin D_3 is abrogated by Snail1 in human colon cancer cells. Endocr Relat Cancer. 2007; 14:141–151. [PubMed: 17395983]
23. Li P, Li C, Zhao X, Zhang X, Nicosia SV, Bai W. p27(Kip1) stabilization and G(1) arrest by 1,25-dihydroxyvitamin D(3) in ovarian cancer cells mediated through down-regulation of cyclin E/cyclin-dependent kinase 2 and Skp1-Cullin-F-box protein/Skp2 ubiquitin ligase. J Biol Chem. 2004; 279:25260–25267. [PubMed: 15075339]
24. Li YC, Pirro AE, Demay MB. Analysis of vitamin D-dependent calcium-binding protein messenger ribonucleic acid expression in mice lacking the vitamin D receptor. Endocrinology. 1998; 139:847–851. [PubMed: 9492012]
25. Lokeshwar BL, Schwartz GG, Selzer MG, Burnstein KL, Zhuang SH, Block NL, Binderup L. Inhibition of prostate cancer metastasis in vivo: a comparison of 1,23-dihydroxyvitamin D (calcitriol) and EB1089. Cancer Epidemiol Biomarkers Prev. 1999; 8:241–248. [PubMed: 10090302]
26. Maruyama R, Aoki F, Toyota M, Sasaki Y, Akashi H, Mita H, Suzuki H, Akino K, Ohe-Toyota M, Maruyama Y, et al. Comparative genome analysis identifies the vitamin D receptor gene as a direct target of p53-mediated transcriptional activation. Cancer Res. 2006; 66:4574–4583. [PubMed: 16651407]
27. Narvaez CJ, Matthews D, LaPorta E, Simmons KM, Beaudin S, Welsh J. The impact of vitamin D in breast cancer: genomics, pathways, metabolism. Front Physiol. 2014; 5:213. [PubMed: 24982636]
28. Narvaez CJ, Simmons KM, Brunton J, Salinero A, Chittur SV, Welsh JE. Induction of STEAP4 correlates with 1,25-dihydroxyvitamin D_3 stimulation of adipogenesis in mesenchymal progenitor cells derived from human adipose tissue. J Cell Physiol. 2013; 228:2024–2036. [PubMed: 23553608]
29. Nickerson T, Huynh H. Vitamin D analogue EB1089-induced prostate regression is associated with increased gene expression of insulin-like growth factor binding proteins. J Endocrinol. 1999; 160:223–229. [PubMed: 9924191]
30. Nieman KM, Kenny HA, Penicka CV, Ladanyi A, Buell-Gutbrod R, Zillhardt MR, Romero IL, Carey MS, Mills GB, Hotamisligil GS, et al. Adipocytes promote ovarian cancer metastasis and provide energy for rapid tumor growth. Nat Med. 2011; 17:1498–1503. [PubMed: 22037646]
31. Park WH, Seol JG, Kim ES, Binderup L, Koeffler HP, Kim BK, Lee YY. The induction of apoptosis by a combined 1,25(OH) $2D_3$ analog, EB1089 and TGF-beta1 in NCI-H929 multiple myeloma cells. Int J Oncol. 2002; 20:533–542. [PubMed: 11836565]
32. Raja FA, Chopra N, Ledermann JA. Optimal first-line treatment in ovarian cancer. Ann Oncol. 2012; 23(Suppl 10):x118–x127. [PubMed: 22987945]
33. Rangel-Moreno J, Moyron-Quiroz JE, Carragher DM, Kusser K, Hartson L, Moquin A, Randall TD. Omental milky spots develop in the absence of lymphoid tissue-inducer cells and support B and T cell responses to peritoneal antigens. Immunity. 2009; 30:731–743. [PubMed: 19427241]
34. Robert Clark VK, Schoof Michael, Rodriguez Irving, Theriault Betty, Chekmareva Marina, Rinker-Schaeffer Carrie. Milky spots promote ovarian cancer metastatic colonization of peritoneal adipose in experimental models. Am J Pathol. 2013; 183:576–591. [PubMed: 23885715]
35. Roby KF, Taylor CC, Sweetwood JP, Cheng Y, Pace JL, Tawfik O, Persons DL, Smith PG, Terranova PF. Development of a syngeneic mouse model for events related to ovarian cancer. Carcinogenesis. 2000; 21:585–591. [PubMed: 10753190]

Author Manuscript Author Manuscript Author Manuscript Author Manuscript

36. Steinkamp MP, Winner KK, Davies S, Muller C, Zhang Y, Hoffman RM, Shirinifard A, Moses M, Jiang Y, Wilson BS. Ovarian tumor attachment, invasion, and vascularization reflect unique microenvironments in the peritoneum: insights from xenograft and mathematical models. Front Oncol. 2013; 3:97. [PubMed: 23730620]

37. Sung V, Feldman D. 1,25-Dihydroxyvitamin D_3 decreases human prostate cancer cell adhesion and migration. Mol Cell Endocrinol. 2000; 164:133–143. [PubMed: 11026565]

38. Tanaka H, Abe E, Miyaura C, Kuribayashi T, Konno K, Nishii Y, Suda T. 1alpha,25-Dihydroxycholecalciferol and a human myeloid leukaemia cell line (HL-60). Biochem J. 1982; 204:713–719. [PubMed: 6289803]

39. Tsai MJ, O'Malley BW. Molecular mechanisms of action of steroid/thyroid receptor superfamily members. Annu Rev Biochem. 1994; 63:451–486. [PubMed: 7979245]

40. Welsh J. Vitamin D and prevention of breast cancer. Acta Pharmacol Sin. 2007; 28:1373–1382. [PubMed: 17723171]

41. Welsh J. Vitamin D and cancer: integration of cellular biology, molecular mechanisms and animal models. Scand J Clin Lab Invest Suppl. 2012; 243:103–111. [PubMed: 22536770]

42. Zhang L, Yang N, Garcia JR, Mohamed A, Benencia F, Rubin SC, Allman D, Coukos G. Generation of a syngeneic mouse model to study the effects of vascular endothelial growth factor in ovarian carcinoma. Am J Pathol. 2002; 161:2295–2309. [PubMed: 12466143]

43. Zhang X, Jiang F, Li P, Li C, Ma Q, Nicosia SV, Bai W. Growth suppression of ovarian cancer xenografts in nude mice by vitamin D analogue EB1089. Clin Cancer Res. 2005; 11:323–328. [PubMed: 15671562]

44. Zhang X, Li P, Nicosia Bao J, Wang SV, Enkemann H, Bai WSA. Suppression of death receptor-mediated apoptosis by 1,25-dihydroxyvitamin D_3 revealed by microarray analysis. J Biol Chem. 2005; 280:35458–35468. [PubMed: 16093247]

45. Zhang X, Nicosia SV, Bai W. Vitamin D receptor is a novel drug target for ovarian cancer treatment. Curr Cancer Drug Targets. 2006; 6:229–244. [PubMed: 16712459]

Author Manuscript Author Manuscript Author Manuscript Author Manuscript

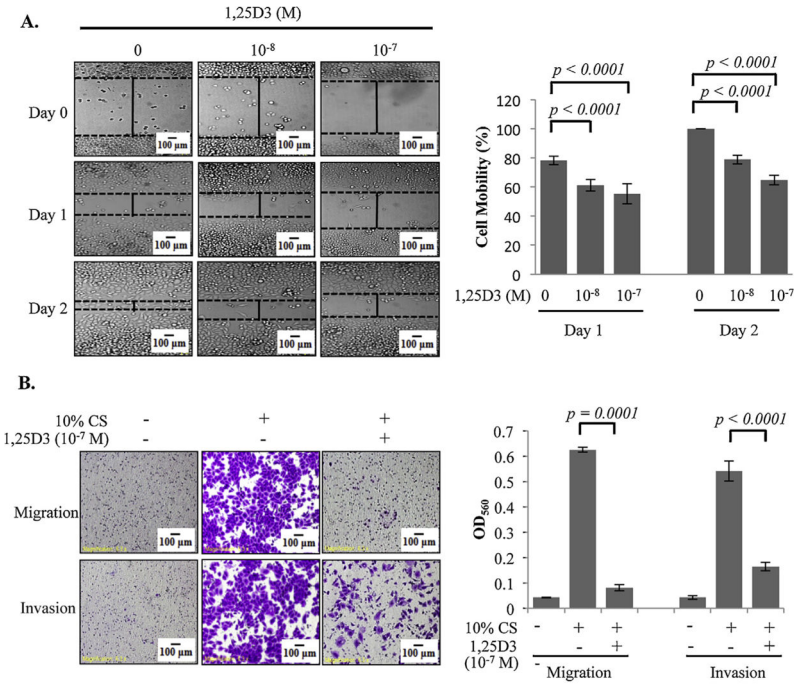

Fig. 1.

Suppression of EOC migration and invasion by $1,25D_3$ in monolayer scratch and transwell assays. (A) *In vitro* monolayer scratch assays. OVCAR3 cells were pre-treated with $1,25D_3$ at indicated concentrations for 6 days. Ethanol (EtOH) was used as the vehicle control. Images of cells at 0, 1 and 2 days after wounding are shown (magnification × 10). The histograms show % cell mobility by imaging analyses as described in Section 2. (B) Transwell migration and invasion assays. 1×10^5 cells of OVCAR3 cells pretreated with EtOH or 10^{-7} M $1,25D_3$ were plated and incubated for 18 h at 37 °C. Cells passing through the Matrigel-coated membrane were stained (left panels) and quantified using a spectrophotometer at OD_{560} (bar graphs). For each data point, triplicate samples were analyzed. The experiments were reproduced twice.

Author Manuscript Author Manuscript Author Manuscript Author Manuscript

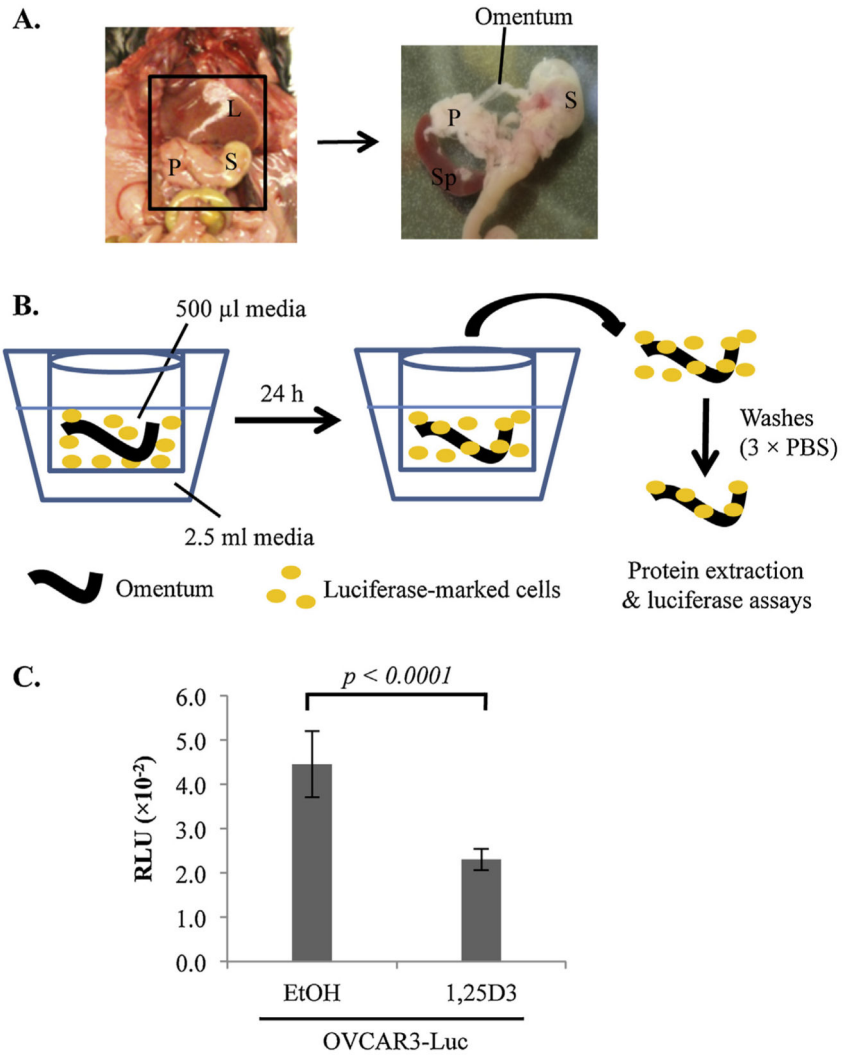

Fig. 2.

Suppression of EOC invasion into omentum by $1,25D_3$ through epithelial VDR in *ex vivo* assays. (A) A schematic diagram showing the location of the murine omentum in the peritoneal cavity between the liver (L), stomach (S), pancreas (P) and spleen (Sp). The right panel shows an enlarged view of the area with the omentum and its position relative to spleen, stomach and pancreas. The omentum was isolated by cutting the omental/pancreatic junction with a scissor. (B) Illustration of the *ex vivo* assay system of co-culturing mouse omenta and luciferase-marked human EOC cells. The omentum is cultured in the apparatus shown, consisting of a Millipore transwell insert containing 500 µl media, placed in a 12-well culture plate containing 2.5 ml media. (C) Suppression of EOC invasion into omenta by $1,25D_3$. OVCAR3-Luc cells were pretreated with EtOH or 10^{-7} M $1,25D_3$ for 6 days. 1×10^6 cells were co-cultured with the omentum for 24 h at 37 °C. For each data point, triplicate samples were analyzed. The experiments were reproduced twice.

Author Manuscript Author Manuscript Author Manuscript Author Manuscript

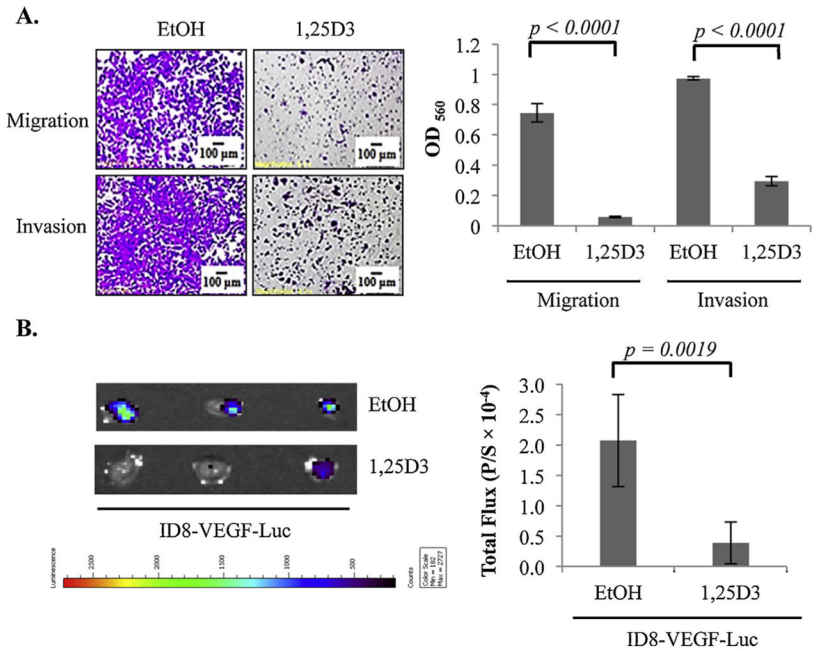

Fig. 3.

Suppression of EOC invasion to the omentum in mice by $1,25D_3$ through the epithelial VDR. (A) Suppression of migration and invasion of mouse epithelial ovarian tumor cells in transwell assays. ID8-VEGF-Luc cells were pre-treated with EtOH or 10^{-7} M $1,25D_3$. Migration and invasion were measured as in Fig. 1 for OVCAR3 cells. (B) Suppression of ID8-VEGF cell invasion into omenta in intact mice by $1,25D_3$ through the epithelial VDR. ID8-VEGF-Luc cells were pretreated with either EtOH or $1,25D_3$ (10^{-7} M) for 6 days. 5×10^6 of treated cells were injected *i.p.* into mice (n = 5/group). After 18 h, omenta were isolated. Bioluminescence IVIS images were captured (left panels) and quantified (bar graphs, *p*/*s* = photons/second). The experiments were reproduced twice.

Author Manuscript Author Manuscript Author Manuscript Author Manuscript

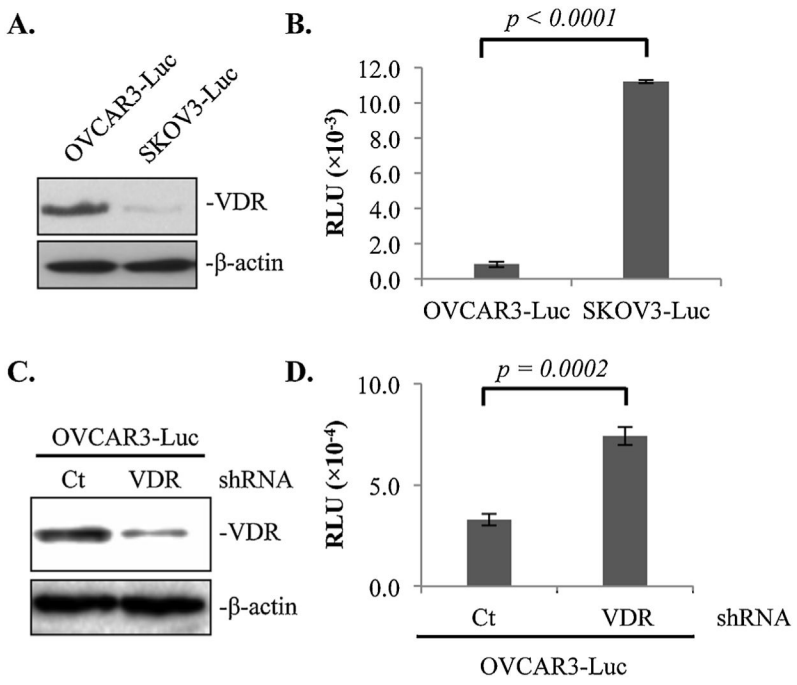

Fig. 4.

$1,25D_3$-independent suppression of EOC invasion to the omentum by epithelial VDR revealed in *ex vivo* assays. (A) Immunoblotting analyses showing VDR protein expression levels in OVCAR3-Luc and SKOV3-Luc cells using β-actin as a loading control. (B) Normalized luciferase activities of OVCAR3-Luc and SKOV3-Luc cells invaded mouse omenta. (C) Immunoblotting analyses showing VDR protein expression levels in OVCAR3-Luc cell stably expressing control (Ct) or VDR (VDR) shRNA using β-actin as a loading control. (D) Normalized luciferase activities of OVCAR3-Luc cells expressing Ct or VDR shRNA invaded mouse omenta. For each data point, triplicate samples were analyzed. The experiments were reproduced twice.

Author Manuscript Author Manuscript Author Manuscript Author Manuscript

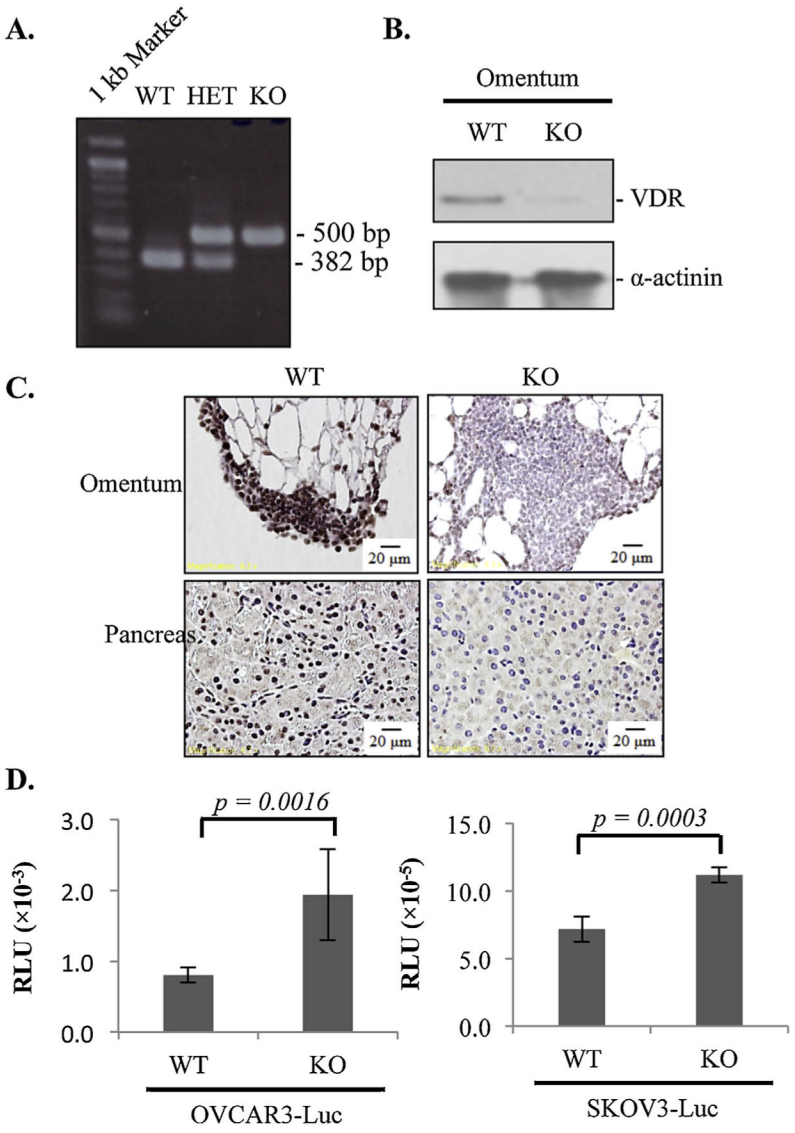

Fig. 5.

Suppression of EOC colonization to the omentum by stromal VDR in *ex vivo* co-culturing assays. (A) Mouse genotyping for wild type (WT), VDR heterozygous (HET) and VDR null (KO) mice. (B) VDR protein levels in omental lysates as determined by immunoblotting analyses. (C) Immunohistochemistry showing VDR protein expression in the omentum and pancreas of WT and KO mice. (D) *Ex vivo* assays showing luciferase activities of OVCAR3-Luc and SKOV3-Luc cells colonized the omentum of WT and KO mice. For each data point, triplicate samples were analyzed. The experiments were reproduced twice.

Author Manuscript Author Manuscript Author Manuscript Author Manuscript

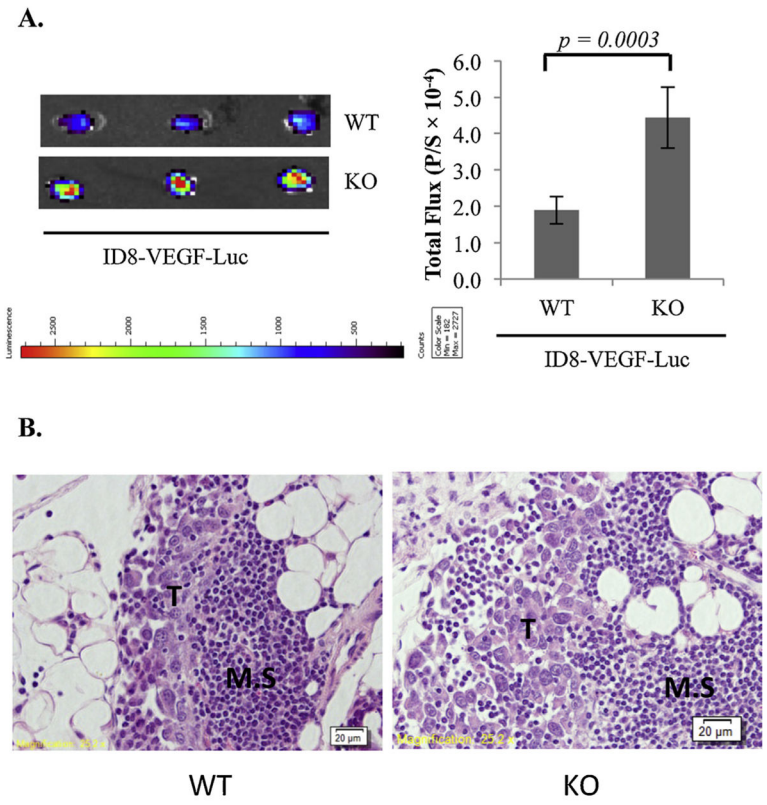

Fig. 6.

Suppression of EOC colonization to the omentum by stromal VDR in the ID8-VEGF syngeneic EOC mouse model. (A) 5×10^6 ID8-VEGF-Luc cells were *i.p.* injected into WT ($n = 5$) and KO ($n = 5$) mice. 18 h later, omenta were isolated and bioluminescence IVIS images of the tumors were captured (left panels) and quantified (bar graphs, *p*/*s* = photons/second). (B) Sections of isolated omenta were subjected to hematoxylin and eosin stain. Tumors (T) established as metastatic are obvious in the milky spots (M.S.).

Author Manuscript Author Manuscript Author Manuscript Author Manuscript

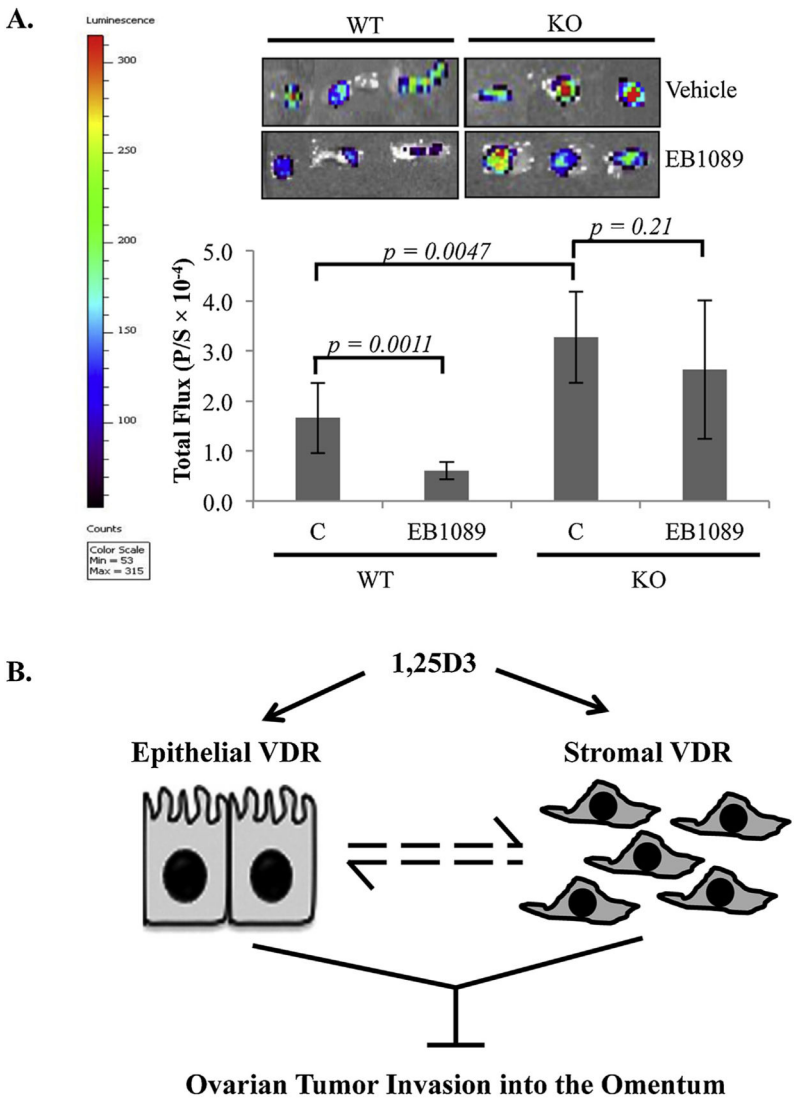

Fig. 7.

Suppression of EOC invasion into omenta of WT and VDR null mice by EB1089 mediated through the stromal VDR. WT and KO mice (n = 6 per group) received *i.p.* injections of 0.5 μg/kg EB1089 in sesame oil (final volume 100 μl) or sesame oil alone (vehicle) every other day for 10 days prior to *i.p.* injection of 5×10^6 ID8-VEGF-Luc cells. (A) Omenta were excised 18 h later and bioluminescence IVIS images were captured (left panels) and quantified (bar graphs, *p*/*s* = photons/second). (B) A schematic diagram showing our working concept that $1,25D_3$ suppresses EOC invasion in the omentum through epithelial and stromal VDR, which there may be crosstalk as indicated by dashed lines. See text for further details.